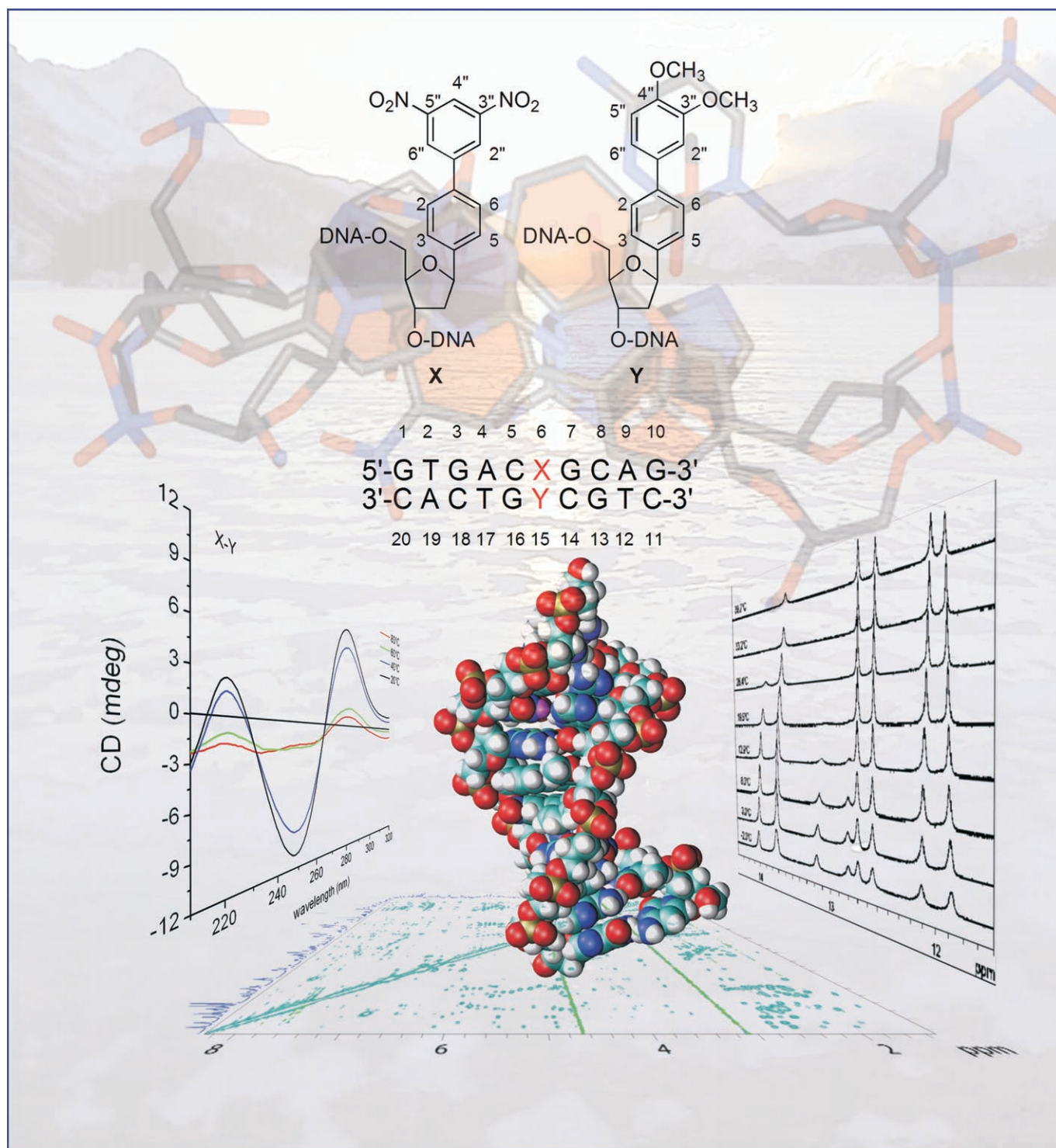


## Solution Structure of a DNA Duplex Containing a Biphenyl Pair

Zeena Johar,<sup>[a]</sup> Alain Zahn,<sup>[b]</sup> Christian J. Leumann,\*<sup>[b]</sup> and Bernhard Jaun\*<sup>[a]</sup>



**Abstract:** Hydrogen-bonding and stacking interactions between nucleobases are considered to be the major noncovalent interactions that stabilize the DNA and RNA double helices. In recent work we found that one or multiple biphenyl pairs, devoid of any potential for hydrogen bond formation, can be introduced into a DNA double helix without loss of duplex stability. We hypothesized that interstrand stacking interactions of the biphenyl residues maintain duplex stability. Here we present an NMR structure of the decamer duplex d(GTGACXGCAG)·

d(CTGCGTTCAC) that contains one such X/Y biaryl pair. X represents a 3',5'-dinitrophenyl- and Y a 3',4'-dimethoxybiphenyl C-nucleoside unit. The experimentally determined solution structure shows a B-DNA duplex with a slight kink at the site of modification. The biphenyl groups are intercalated side by side as a pair between

the natural base pairs and are stacked head to tail in van der Waals contact with each other. The first phenyl rings of the biphenyl units each show tight intrastrand stacking to their natural base neighbors on the 3'-side, thus strongly favoring one of two possible interstrand intercalation structures. In order to accommodate the biphenyl units in the duplex the helical pitch is widened while the helical twist at the site of modification is reduced. Interestingly, the biphenyl rings are not static in the duplex but are in dynamic motion even at 294 K.

**Keywords:** DNA structures · hydrophobic bases · interstrand stacking · NMR spectroscopy · nucleic acids

## Introduction

Hydrogen-bonding and stacking interactions between nucleobases are the major components of the noncovalent forces that stabilize the DNA and RNA double helices.<sup>[1,2]</sup> The relative contribution of each to this stability has been controversial since the discovery of the double helix. Recent experimental data on oligonucleotide duplexes containing nonpolar nucleobase substitutes as dangling ends fueled this discussion.<sup>[3,4]</sup> Factors such as hydrophobicity ( $\log P$ ), polarizability, dipole moment, surface area, and stacking area have been discussed as contributors to the observed enhanced thermodynamic stabilities of these capped oligodeoxynucleotide duplexes.<sup>[4-6]</sup> Shape mimics of complementary natural bases that are devoid of any possibility to form hydrogen bonds have recently been used to probe DNA-processing enzymes. Although such isosteres destabilize DNA duplexes, they can code for each other with high precision in DNA polymerase-mediated replication.<sup>[7-13]</sup> These findings triggered an extensive search for hydrophobic, aromatic pairs that are orthogonal to the natural base pairs in their recognition properties.<sup>[14-24]</sup> Such pairs are of interest for extension of the genetic alphabet.


A solution structure of a duplex containing a 4-methylbenzimidazole/difluorotoluene base pair showed that shape-

complementary hydrophobic base analogues are located side by side in the base stack of the duplex without distorting the overall conformation of the DNA backbone.<sup>[25]</sup> This aromatic pair, however, destabilizes the duplex. One of the first examples of a stabilizing pair lacking hydrogen bonds was the pyrene/abasic site pair.<sup>[6,12]</sup> Also in this case, the overall geometry is only marginally affected by the modification.<sup>[26]</sup> The enhanced stability is believed to originate from extensive stacking interactions between the pyrene unit and the nearest neighbor natural base pairs. During review of this communication an X-ray structure of a duplex containing a *m*-fluorobenzene self-pair and an NMR structure of a duplex containing a propynylisocarbostyryl (PICS) self-pair were reported.<sup>[27]</sup> In the former duplex, a side-by-side arrangement of the *m*-fluorobenzene residues with no major structural perturbations from B-DNA was observed. The latter duplex showed the PICS self-pair in an interstrand intercalation arrangement.

DNA is becoming increasingly important as a scaffold for the self-assembly of attached molecular entities on the nanometer scale<sup>[28]</sup> and also as a functional molecule, due to the charge-transport properties through the DNA base stack.<sup>[29]</sup> In our research directed towards the exploitation of interstrand aromatic stacking interactions for production of novel and functional DNA duplex architectures we recently found that up to seven biphenyl C-nucleoside pairs can be accommodated in a helix without loss of duplex stability.<sup>[30,31]</sup> From molecular modeling we proposed a zipper-like recognition motif, assuming that the stability is based on interstrand aromatic interactions between the biphenyl residues. Such a zipper motif has previously been shown by NMR spectroscopy to exist in unusual 5'-(GXA)/(AYG)-5' DNA sequence motifs (X/Y = T/A, A/T, C/G, G/C, and G/G).<sup>[32]</sup> Here we describe an NMR solution structure of an oligodeoxynucleotide duplex containing a 3',5'-dinitrophenyl/3',4'-dimethoxybiphenyl (X/Y) base pair (Scheme 1).

[a] Z. Johar, Prof. B. Jaun  
Laboratory of Organic Chemistry, ETH Zürich  
Wolfgang-Pauli-Strasse 10, 8093 Zürich (Switzerland)  
Fax: (+41) 44-632-1475  
E-mail: jaun@org.chem.ethz.ch

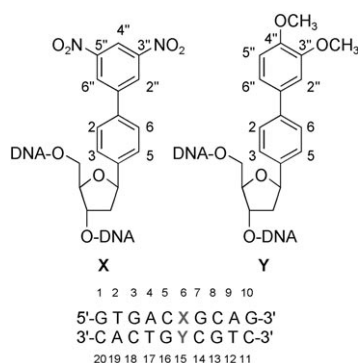
[b] A. Zahn, Prof. C. J. Leumann  
Department of Chemistry and Biochemistry  
University of Bern  
Freiestrasse 3, 3012 Bern (Switzerland)  
Fax: (+41) 31-631-3422  
E-mail: leumann@ioc.unibe.ch

 Supporting information for this article is available on the WWW under <http://www.chemeurj.org> or from the author.

## Results and Discussion

The thermal duplex stability of the modified duplex was determined by UV melting curve analysis (Figure 1). For comparison, the same experiment was also performed with an unmodified duplex containing an A/T base pair instead of the biphenyl modifications. We found  $T_m$  values of 50.1°C for the modified duplex and 45.2°C for the duplex in which X/Y is replaced by A/T. This clearly shows an enhanced thermal stability of the biphenyl base pair over an A/T base pair, by 4.9°C. We find that the total hyperchromicity is lower in the case of the modified duplex. This may be a direct consequence of differences in induced dipolar interactions between the modified and the natural bases.

To elucidate the origin of the higher thermal stability, the free energies of duplex formation ( $\Delta G^{25^\circ\text{C}}$ ) were derived from plots of  $1/T_m$  against  $\ln c$  for the biphenyl and the natural duplex, assuming that the two-state melting mechanism is fulfilled in both cases (Figure S3, Supporting Information). As expected, we found higher thermodynamic stability of the modified X/Y ( $\Delta G^{25^\circ\text{C}} = -15.2 \text{ kcal mol}^{-1}$ ) over the A/T duplex ( $\Delta G^{25^\circ\text{C}} = -13.2 \text{ kcal mol}^{-1}$ ), by  $2 \text{ kcal mol}^{-1}$ . Interestingly, the higher thermodynamic stability is largely due to a more favorable pairing enthalpy term ( $\Delta H$ ), which amounts to  $-79.9 \text{ kcal mol}^{-1}$  for the X/Y and to  $-69.8 \text{ kcal mol}^{-1}$



Scheme 1. Chemical structures of the biphenyl-C-nucleoside derivatives and sequence information on the duplex investigated.

$\text{mol}^{-1}$  for the A/T duplex. This finding is in agreement with (but no proof of) an enhanced contribution of stacking interactions to the stability in the modified duplex.

Preliminary structural investigations of both the modified and the unmodified duplex were performed by CD spectroscopy (Figure S4, Supporting Information). No significant differences in shape and ellipticity maxima and minima were found. CD spectroscopy thus points to only minor deviations from the B-type conformation in the modified duplex. No further structural information around the site of modification was deducible from the CD spectra.

A study of the temperature dependence of the  $1\text{D}^{-1}\text{H}$  spectrum (Figure S1, Supporting Information) revealed that below around 290 K some lines—in particular those in the

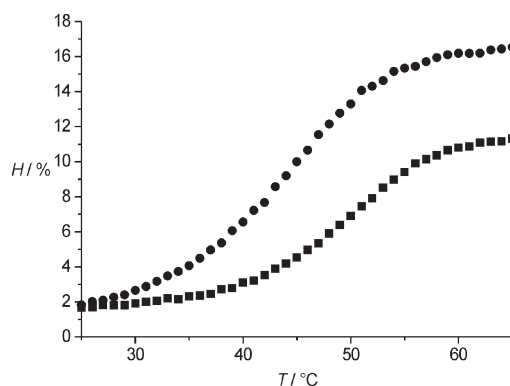


Figure 1. UV melting curves of modified and unmodified duplex decamers ■: X/Y, ●: A/T.

region where the protons of the biphenyl moieties are expected—broadened and did not sharpen again when the temperature was lowered down to the experimental limit (freezing of the sample). This was attributed to a dynamic process different from what is seen in duplex melting/formation, its rate approaching the NMR timescale below 300 K (see discussion below). We therefore decided to carry out the full NMR analysis at the intermediate temperature of 294 K, where the lines were comparably sharp and not yet affected by the dynamics of melting.

The residue-specific assignment of all sugar protons, except for some of the strongly overlapping  $\text{H}_2\text{C}(5')$  groups, and of all base protons was possible through a combination of COSY, NOESY, HSQC, and HMBC spectroscopy. Beginning at the four ends, the pattern of NOEs between the base and sugar protons along each strand allowed the sequential assignment to be performed and already qualitatively indicated that the overall conformation is similar to that of B-type DNA. A list of assignments of the  $^1\text{H}$  resonances from the spectra in  $\text{D}_2\text{O}$  and in  $\text{H}_2\text{O}/\text{D}_2\text{O}$  9:1 is given in Table 1, and the position numbering of the two biphenyl base analogues is shown in Scheme 1.

If the rotation of the biphenyl rings around their axes were slow on the NMR timescale, one would clearly expect two sets of resonances for biphenyl protons that are rotationally equivalent, such as H3/H5, H2/H6 (and, in the dinitrobiphenyl moiety, also H2''/H6'') in the highly asymmetric environment of the duplex. That only one set of time-averaged resonances was observed shows that the three symmetrical rings rotate more rapidly than the NMR timescale inside the duplex at 294 K. We presume the same for the asymmetrically substituted dimethoxyphenyl ring (see below), although in this case the observation of a single set of resonances would also be consistent with a single predominant rotamer.

Only five of the nine possible imino protons were observed in the  $\text{H}_2\text{O}/\text{D}_2\text{O}$  9:1 spectra at 294 K. They could be assigned through their NOEs to the four nonterminal G–C base pairs and the central A4–T17 pair (Table 1). While it is common that the imino protons of terminal base pairs can be too broad to be detected at this temperature, and the



second-last base pairs are often also not detected if they are A–T pairs, the fact that the A4–T17 imino proton is broadened indicates an unusually high rate of exchange for this pair in the inner part of the sequence. At 271 K, the exchange with solvent protons is slow enough to allow detection of all nine imino protons, although the signals of the two outermost base pairs are still quite broad.

Qualitative inspection of the overall NOE pattern and analysis of the vicinal coupling constants in the ribose units revealed that the duplex is a B-type helix with the sugar units, including the two biphenyl-substituted residues, predominantly in the *C2'-endo* conformation. A considerable number of NOEs between the biphenyl moieties and residues on the opposite strand, between the biphenyls and their neighboring nucleotides, and also between the two biphenyl units themselves were observed (Figure 2). Together with large high-field shifts of several of the biphenyl signals (see, for example, the chemical shift of the 3''-methoxy signal at 2.65 ppm), as compared to the spectra of the mononucleosides, this shows that the biphenyl units must be reaching across to the opposite strands and that they are intercalated into the stack of the base pairs.

For simulated annealing calculations of structures that are consistent with the experimental constraints, the ambiguity introduced by the rotational averaging in the symmetrical phenyl rings precluded, at first, the use of the corresponding restraints. Nevertheless, the ensemble of unambiguous NOEs defined the structure sufficiently well to allow resolution of the ambiguity for some of these NOEs and their re-introduction into the calculations in a cyclic refinement. A set of conflicting NOEs remained, however, in particular with regard to the asymmetrically substituted 3'',4''-dimethoxyphenyl ring. This indicates that this ring, like the others, rotates at 294 K, but the rotamer with the 3''-methoxy group

pointing in the direction of the minor groove is clearly dominant.

Figure 3a shows a bundle of (calculated) low-energy structures from the larger ensemble of accepted structures with no NOE violations (with exclusion of a few still ambiguous NOEs), generated by the simulated annealing calculation with the NOE constraints. A single representative structure

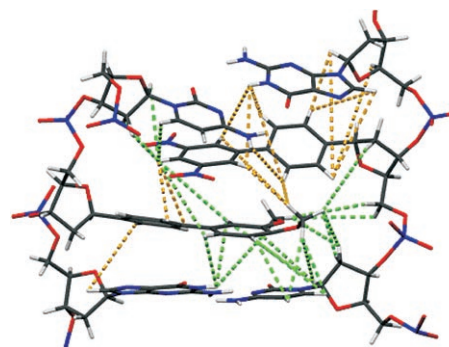


Figure 2. NOEs observed between the biphenyl moieties and between biphenyl residues, neighboring bases, and the backbone sugars (green: unambiguous NOEs; yellow: NOEs that are ambiguous with respect to two rotationally equivalent, dynamically averaged protons).

is represented in stereo in Figure 3b.

The overall conformation is that of an antiparallel Watson–Crick B-DNA-like double helix with a less helical region around the biphenyl units and varying degrees of overall bending. The biphenyl groups are intercalated side by side as a pair between the natural base pairs and are stacked head to tail in van der Waals contact with each other and with their respective neighboring base pairs. The first phenyl rings (C1–C6) are tightly stacked against the

Table 1.  $^1\text{H}$  chemical shifts and assignments (R = residue).

R	Ribose protons							Nucleobase protons					Biphenyl units					NH protons ( $\text{H}_2\text{O}$ )						
	H1'	H2'1	H2'2	H3'	H4'	C5'1	C5'2	H2	H5	Me-5	H6	H8	H2/H6	H3/H5	H2''/6''	H4''	H5''	MeO-3''	MeO-4''	HN1	HN3	HN41	HN42	
G1	5.88	2.68	2.49	4.71	4.12	3.6	3.63					7.83												
T2	5.71	2.37	2.03	4.78	4.10	na	na			1.26	7.20													
G3	5.49	2.67	2.56	4.90	4.23	na	na					7.76								12.43				
A4	6.07	2.74	2.42	4.92	4.32	4.10	na	7.63				7.95												
C5	5.61	2.27	2.16	4.80	4.01	4.07	na		4.99		7.12											7.54	6.18	
X6	4.73	2.52	1.84	4.72	4.18	3.89	3.83						6.88	6.90	7.87	7.67								
G7	5.44	2.39	2.50	4.82	4.24	na	na					7.77								11.83				
C8	5.53	2.18	1.83	4.74	4.07	na	na		5.34		7.30											8.05	6.19	
A9	5.90	2.16	2.59	4.90	4.24	na	na	7.68				8.07												
G10	5.90	2.75	2.35	4.52	4.05	na	na					7.61												
C11	5.80	2.60	1.98	4.57	3.99	3.67	3.63		5.80		7.68													
T12	5.63	2.38	2.11	4.76	4.06	na	na			1.55	7.36													
G13	5.80	2.60	2.45	4.87	4.24	3.93	3.87					7.71								12.60				
C14	5.71	2.46	2.20	4.84	3.99	na	na		5.11		7.20											7.72	6.45	
Y15	4.51	2.42	1.82	4.65	3.91	na	4.10						6.56	6.51	6.37/5.97		6.16	2.65	3.45					
G16	5.53	2.17	2.50	4.81	4.22	4.10	4.02													11.97				
T17	5.91	2.36	2.04	4.74	4.12	na	na			1.20	7.14											13.51		
C18	5.48	2.27	1.94	4.72	3.99	na	na		5.57		7.41											8.35	6.70	
A19	6.12	2.75	2.56	4.90	4.28	na	na	7.67				8.16												
C20	5.94	2.02	2.00	4.35	3.88	4.14	3.94		5.23		7.23													

neighboring base in the same strand in the 3'-direction (Figure 3c). In all accepted structures, the order of intercalation is the same: the dinitrobiphenyl moiety is nearer to the G10–C11 end of the duplex, whereas the dimethoxybiphenyl group is on the G1–C20 side.

The side-by-side intercalation of two aromatic residues where only one base pair would be located in a natural B-DNA helix requires stretching of the backbone through changes in the dihedral angles near the biphenyl residues. Experimentally, this could be detected for the H5' and H5'' protons of the 3',5'-dinitrobiphenyl residue: in contrast to the H5' and H5'' protons of the residues in the natural part of the duplex, which show the pattern of NOEs typical for B-DNA, the H<sub>2</sub>C(5')-group of X6 is turned towards the center of the helix and shows medium to strong NOEs to the 3'-methoxy group and H2'/H2'' of C5. The dihedral angle  $\gamma$  of X6 is  $g^-$ , as compared to  $g^+$  for B-DNA. In all ac-

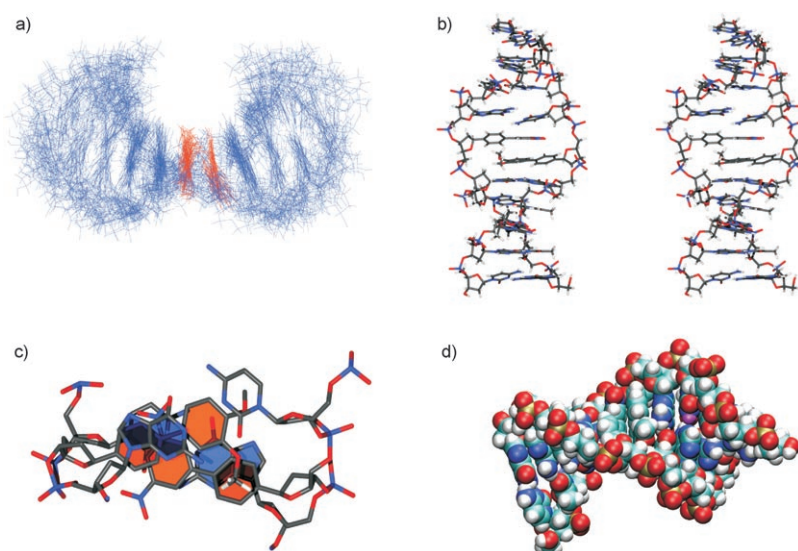


Figure 3. a) Superposition of the 20 structures with lowest calculated energies out of a set of 75 accepted structures. The superposition is based on all phosphorus atoms except the terminal ones in each strand. b) Stereoview of a representative single structure from the set shown in a). c) Section of the duplex with the biphenyl residues and their neighboring base pairs, highlighting the stacking interactions (view direction perpendicular to the mean base pair plane). d) Space-filling view of the structure in b) illustrating the van der Waals contact between the biphenyl units and with their neighboring base pairs, the widening of the minor groove, and the resulting exposure of the A4–T17 imino proton (colored in magenta).

cepted structures the corresponding dihedral angle  $\gamma$  of the dimethoxybiphenyl residue Y15 is  $t$ , but we do not have direct experimental evidence from coupling constants. Unfortunately, severe overlap in the H5'/H5''/H4' region of the spectrum did not allow us to assign all H<sub>2</sub>C(5') protons, and no reliable  $J_{H4',H5'}$  coupling constants could be extracted, except in the case of X6 and the 5'-terminal residues. We were therefore unable to carry out a more detailed analysis of the backbone deformation in the biphenyl region. This lack of dihedral constraints, in particular for the phosphodiester linkages, causes a variation in the overall bending of the duplex that manifests itself as a "fraying out" towards the ends of the structural bundle in Figure 3a.

The extra space needed by the additional aromatic residue in the stack leads to a reduced helical twist: the twist between the flanking G7–C14 and C5–G16 base pairs is only around 35°. Therefore, over three aromatic stacking distances of around 3.6 Å each, the total twist is only as much as normally observed between two adjacent base pairs. This leads to a pronounced widening of the minor groove (Figure 3d), and the concomitant exposure of the A4–T17 base pair may well be the reason for the unusually fast exchange of its imino proton (colored in magenta in Figure 3d).

## Conclusion

The experimentally determined solution structure shows that a B-type DNA duplex can accommodate two opposing biphenyl base analogues through local widening of the pitch and reduction of the twist of the helix. The steric demand of the two biphenyl groups, both of which exclusively point towards the inside of the duplex and have to avoid each other, leads to a particularly tight stacking of their first benzene rings against the natural base neighbor on the 3'-side, thus selecting one of two possible interstrand intercalation geometries. The two phenyl rings of the biphenyl units are nearly planar and stack on each other, producing an uninterrupted base-stack throughout the double helix. Both biphenyl units span the whole of their adjacent natural base pairs and have the strongest interresidue  $\pi$  interactions between the distal ring of one unit and the proximal ring of the opposite unit. The increased stacking surface to a complete neighboring natural base pair, together with the interbiphenyl contacts, fully explains the observed high thermodynamic stability of this duplex. Of special interest are the rotational dynamics along the biphenyl axes, which are not frozen even at 271 K. This points to considerable dynamics of the duplex structure but does not preclude the stacked arrangement being the preferred conformational state. Although the detailed mechanism of rotation (in-stack against out-of-stack) is not known at this point it is worthwhile to consider that the thickness of a phenyl ring is not that much different from its diameter and that it thus resembles an ellipsoid body (squeezed cylinder) more than it does a flat tile.

The structure described here is fully supportive of our proposed zipper recognition motif. We found earlier that not only one but multiple biphenyl pairs can be introduced into the center of a double helix without loss of helix stability.<sup>[30]</sup> It now remains to be shown whether the observed local biphenyl geometry in this duplex can be extrapolated to several consecutive biphenyl pairs in a duplex. In any case, the thermal stability data of the duplex described here, together with its structure, demonstrate the tolerance of this recognition motif for variation of substituents on the biphenyl periphery. With this, fine tuning of the electronic and recognition properties of the aromatic systems seems possible. This in turn might be of importance in applications in the field of DNA materials, as well as in DNA diagnostics.

## Experimental Section

**Sample preparation:** The syntheses of modified phosphoramidite monomers and their incorporation into oligodeoxynucleotides are described elsewhere.<sup>[33]</sup> Unmodified oligodeoxynucleotides were purchased from Microsynth (Balgach, Switzerland) and used without further purification.

**Thermal denaturation:** All UV melting curves were recorded at 260 nm on a Cary 3E UV/VIS spectrometer (Varian) fitted with a Peltier block and with the aid of Varian WinUV software. The oligonucleotide concentration was 1.2  $\mu\text{M}$  in  $\text{NaH}_2\text{PO}_4$  (10 mM), NaCl (150 mM), pH 7.0. Consecutive heating-cooling-heating cycles over the temperature interval of 10 to 90 °C were applied with a linear gradient of 0.5 °C min<sup>-1</sup>. Heating and cooling ramps were superimposable. Each  $T_m$  value was defined as the maximum of the first derivative of the melting curve. To elucidate thermodynamic data,  $T_m$  measurements were performed at five different concentrations over the range of 0.5–15  $\mu\text{M}$  duplex. Free energy values were then calculated from van't Hoff plots by plotting  $1/T_m$  against  $\ln c$  (Figure S3: Supporting Information).

**NMR spectroscopy:** 1D-<sup>1</sup>H, 1D-<sup>31</sup>P, and 2D NMR-COSY with <sup>31</sup>P decoupling, NOESY with mixing times of 300 msec, 150 msec (Figure S2, Supporting Information), and 75 msec, HSQC, and HMBC spectra were recorded in a 5 mm Shigemi tube with a sample concentration of  $c = 3.1 \text{ mM}$  in  $\text{D}_2\text{O}/\text{Na}$  arsenate buffer (pH 7, 50 mM) at 294 K at 600 MHz (<sup>1</sup>H) and 125 MHz (<sup>13</sup>C). To detect the exchangeable protons, the sample was lyophilized and measured again in  $\text{H}_2\text{O}/\text{D}_2\text{O}$  9:1 Na arsenate (50 mM). The same set of 1D-<sup>1</sup>H and homonuclear 2D spectra were recorded as in  $\text{D}_2\text{O}$ , but with excitation sculpting for suppression of the solvent signal.

Assignment and volume integration of NOESY cross peaks (mixing times 300 ms, 150 ms, and 75 ms, for both the  $\text{D}_2\text{O}$  and  $\text{H}_2\text{O}$  spectra) were performed with the aid of SPARKY.<sup>[34]</sup> Distance constraints and error limits were generated from build-up curves of cross-peak volumes by calibration with known distances ( $\pm 20\%$  error limits) through a python extension within SPARKY.

**Structure calculations:** The simulated annealing molecular dynamics calculations were performed with XPLOR-NIH version 2.16.0.<sup>[35]</sup> The parameter file *parnah1er1\_mod\_new.inp* and the topology file *topall dna.hdg* were modified to deal with the two new DNA base analogues (equilibrium values for bond lengths and angles were based on an X-ray structure of biphenyl).<sup>[36]</sup> All the other parameters concerning the base and the sugar atoms, as well as the force constants ( $k_{\text{bond}} = 1000 \text{ kcal mol}^{-1}$ ,  $k_{\text{angle}} = 500 \text{ kcal mol}^{-1}$ ,  $k_{\text{improper}} = 500 \text{ kcal mol}^{-1}$ ) were left unchanged. For generating a starting structure a “dummy” pdb file was generated by use of a perl script and was then used as a template for generating the structure (.psf) file. The “zero coordinate” pdb files were minimized in order to generate the two single-strand structures at 300 K. The two minimized single strands were then combined into a duplex by introducing hydrogen bond restraints for the Watson–Crick pairs, for which

the imino proton resonances indicated the presence of hydrogen bonds in an otherwise unrestrained simulating annealing calculation. The resulting extended zigzag duplex conformations in which the two biphenyl groups were not stacked and pointed outwards from the duplex were used as starting structures. The simulated annealing (SA) protocol (adopted from the torsional angle dynamics protocol of Stein et al.<sup>[37]</sup>) included 4000 steps (0.015 ps each) of high-temperature torsional angle dynamics at 20000 K, followed by 4000 (0.015 ps) steps of slow cooling to 1000 K with torsional angle dynamics, 2000 steps (0.003 ps) of slow cooling with Verlet dynamics to 300 K, followed by a final Powell minimization. Distance restraints derived from NOESY (as explained above) were introduced in the SA calculation (Table S1, Supporting Information).

Since analysis of the chemical shifts of the imino protons in the  $\text{H}_2\text{O}/\text{D}_2\text{O}$  9:1 1D-spectrum at  $-2^\circ$  indicated the presence of all nine possible base pairs and NOESY in  $\text{H}_2\text{O}/\text{D}_2\text{O}$  9:1 at 295 K indicated Watson–Crick pairing for all base pairs except the two outermost ones, hydrogen bond constraints defining standard Watson–Crick pairing for all base pairs except for the nonnatural base analogues were introduced. For the two base pairs flanking the biphenyl residues this restraint was loosened by 20%. Calculations were performed once without and once with planarity restraints for the base pairs not flanking the biphenyl groups. Introduction of planarity restraints gave bundles with less variation in the propeller twist and buckle of base pairs but otherwise did not change the overall conformation and relative orientation of the biphenyl groups. The only non-bonded interactions used were van der Waals repel functions. A total of 97 structures were generated by use of the SA protocol explained above. Out of these, 75 structures were accepted. Final structures were accepted if they showed no NOE violation  $> 0.1 \text{ \AA}$  and no deviation from equilibrium bond lengths, angles, and impropers of  $> 0.05 \text{ \AA}$ ,  $> 5.0^\circ$ , and  $> 1.5^\circ$ , respectively.

## Acknowledgements

A.Z. and C.J.L. thank the Swiss National Science Foundation (grant-No.: 200020-107692), and Z.J. and B.J. thank the ETH-Zürich (Project No. TH-17/02-4) for financial support.

- [1] C. R. Cantor, P. R. Schimmel, *Biophysical Chemistry Part III: The behavior of biological molecules*, W. H. Freeman, New York, **1980**, pp. 1109–1181.
- [2] W. Saenger, *Principles of Nucleic Acid Structure*, Springer, New York, **1984**.
- [3] K. M. Guckian, B. A. Schweitzer, R. X.-F. Ren, C. J. Sheils, P. L. Paris, D. C. Tahmassebi, E. T. Kool, *J. Am. Chem. Soc.* **1996**, *118*, 8182–8183.
- [4] K. M. Guckian, B. A. Schweitzer, R. X.-F. Ren, C. J. Sheils, P. L. Paris, D. C. Tahmassebi, E. T. Kool, *J. Am. Chem. Soc.* **2000**, *122*, 2213–2222.
- [5] B. A. Schweitzer, E. T. Kool, *J. Am. Chem. Soc.* **1995**, *117*, 1863–1872.
- [6] T. J. Matray, E. T. Kool, *J. Am. Chem. Soc.* **1998**, *120*, 6191–6192.
- [7] S. Moran, R. X.-F. Ren, E. T. Kool, *Proc. Natl. Acad. Sci. USA* **1997**, *94*, 10506–10511.
- [8] K. M. Guckian, J. C. Morales, E. T. Kool, *J. Org. Chem.* **1998**, *63*, 9652–9656.
- [9] J. C. Morales, E. T. Kool, *Nat. Struct. Biol.* **1998**, *5*, 950–954.
- [10] J. C. Delaney, P. T. Henderson, S. A. Helquist, J. C. Morales, J. M. Essigmann, E. T. Kool, *Proc. Natl. Acad. Sci. USA* **2003**, *100*, 4469–4473.
- [11] E. T. Kool, J. C. Morales, K. M. Guckian, *Angew. Chem.* **2000**, *112*, 1046–1068; *Angew. Chem. Int. Ed.* **2000**, *39*, 990–1009.
- [12] T. J. Matray, E. T. Kool, *Nature* **1999**, *399*, 704–708.
- [13] K. M. Guckian, T. R. Krugh, E. T. Kool, *Nat. Struct. Biol.* **1998**, *5*, 954–959.

- [14] M. Berger, A. K. Ogawa, D. L. McMinn, Y. Q. Wu, P. G. Schultz, F. E. Romesberg, *Angew. Chem.* **2000**, *112*, 3069–3071; *Angew. Chem. Int. Ed.* **2000**, *39*, 2940–2942.
- [15] M. Berger, S. D. Luzzi, A. A. Henry, F. E. Romesberg, *J. Am. Chem. Soc.* **2002**, *124*, 1222–1226.
- [16] D. L. McMinn, A. K. Ogawa, Y. Q. Wu, J. Liu, P. G. Schultz, F. E. Romesberg, *J. Am. Chem. Soc.* **1999**, *121*, 11585–11586.
- [17] A. K. Ogawa, Y. Q. Wu, D. L. McMinn, J. Liu, P. G. Schultz, F. E. Romesberg, *J. Am. Chem. Soc.* **2000**, *122*, 3274–3287.
- [18] E. L. Tae, Y. Q. Wu, G. Xia, P. G. Schultz, F. E. Romesberg, *J. Am. Chem. Soc.* **2001**, *123*, 7439–7440.
- [19] C. Yu, A. A. Henry, F. E. Romesberg, P. G. Schultz, *Angew. Chem.* **2002**, *114*, 3997–4000; *Angew. Chem. Int. Ed.* **2002**, *41*, 3841–3844.
- [20] S. Atwell, E. Meggers, G. Spraggon, P. G. Schultz, *J. Am. Chem. Soc.* **2001**, *123*, 12364–12367.
- [21] Y. Wu, A. K. Ogawa, M. Berger, D. L. McMinn, P. G. Schultz, F. E. Romesberg, *J. Am. Chem. Soc.* **2000**, *122*, 7621–7632.
- [22] S. Matsuda, A. A. Henry, P. G. Schultz, F. E. Romesberg, *J. Am. Chem. Soc.* **2003**, *125*, 6134–6139.
- [23] T. Mitsui, A. Kitamura, M. Kimoto, T. To, A. Sato, I. Hirao, S. Yokoyama, *J. Am. Chem. Soc.* **2003**, *125*, 5298–5307.
- [24] I. Hirao, M. Kimoto, T. Mitsui, T. Fujiwara, R. Kawai, A. Sato, Y. Harada, S. Yokoyama, *Nat. Methods* **2006**, *3*, 729–735.
- [25] K. M. Guckian, T. R. Krugh, E. T. Kool, *J. Am. Chem. Soc.* **2000**, *122*, 6841–6847.
- [26] S. Smirnov, R. J. Matray, E. T. Kool, C. Santos, *Nucleic. Acids Res.* **2002**, *30*, 5561–5569.
- [27] S. Matsuda, J. D. Fillo, A. A. Henry, P. Rai, S. J. Wilkens, T. J. Dwyer, B. H. Geierstanger, D. E. Wemmer, P. G. Schultz, G. Spraggon, F. E. Romesberg, *J. Am. Chem. Soc.* **2007**, *129*, 10466–10473.
- [28] N. C. Seeman, *Nature* **2003**, *421*, 427–431.
- [29] M. A. O'Neill, J. K. Barton, in *Topics in Current Chemistry: Electron Transfer in DNA I*, Vol. 236, (Ed.: G. B. Schuster), Springer, **2004**, pp. 67–115.
- [30] C. Brotschi, C. J. Leumann, *Angew. Chem.* **2003**, *115*, 1694–1697; *Angew. Chem. Int. Ed.* **2003**, *42*, 1655–1658; see also accompanying paper: A. Zahn, C. J. Leumann, *Chem. Eur. J.*, **2008**, *14*, 1087–1094.
- [31] C. Brotschi, G. Mathis, C. J. Leumann, *Chem. Eur. J.* **2005**, *11*, 1911–1923.
- [32] S.-H. Chou, K.-H. Chin, *J. Mol. Biol.* **2001**, *312*, 753–768.
- [33] A. Zahn, C. J. Leumann, *Bioorg. Med. Chem.* **2006**, *14*, 6174–6188.
- [34] T. D. Goddard, D. G. Kneller, Program SPARKY v3.110, UCSF, **2004**.
- [35] C. D. Schwieters, J. J. Kuszewski, N. Tjandra, G. M. Clore, *J. Magn. Reson.* **2003**, *160*, 65–73.
- [36] T. Hokelek, S. Dincer, E. Kilic, *Cryst. Res. Technol.* **2002**, *37*, 1138–1142.
- [37] E. G. Stein, L. M. Rice, A. T. Brünger, *J. Magn. Reson.* **1997**, *124*, 154–164.

Received: August 22, 2007  
Published online: November 23, 2007